ACADEMIA ROMÂNĂ
Revue Roumaine de Chimie
https://www.icf.ro/rrch/

Rev. Roum. Chim.,
2023, *68*(3–4), 143–151
DOI: 10.33224/rrch.2023.68.3-4.04

Dedicated to Dr. Maria Zaharescu
on the occasion of her 85th anniversary

STUDY OF COBALAMIN ADDUCTS WITH CYSTEINE AND ITS OXIDIZED SULFENIC, SULFINIC AND SULFONIC DERIVATIVES

Artiom GAINA-GARDIUTA,[a] Alexandru LUPAN,[a] Adrian M.V. BRÂNZANIC[b] and Radu SILAGHI-DUMITRESCU[a,*]

[a] Department of Chemistry, Babeș-Bolyai University, Str. Arany Janos Nr. 11, RO-400028 Cluj-Napoca, Roumania
[b] Raluca Ripan Institute for Research in Chemistry, Babeș-Bolyai University, Fantanele 30, 400294, Cluj-Napoca, Roumania

Received December 29, 2022

In this paper, the reactivity of cobalamin towards S-oxidized cysteine derivatives (sulfenic, sulfinic, sulfonic and S-sulfate) is analyzed and compared to the reactivity towards related nitrogen, oxygen and sulfur-based ligands, focusing on the concept of linkage isomerism. UV-Vis spectra complemented by DFT and TD-DFT calculations show that cysteine and its oxidized derivatives do yield adducts, with a preference for binding to the cobalt through the sulfur.

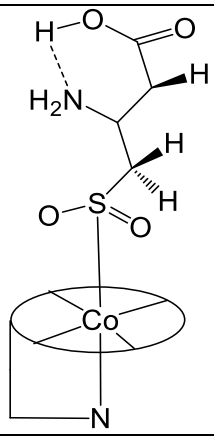

INTRODUCTION

Vitamin B_{12} or cobalamin (Cbl, Fig. 1) is the only vitamin that contains a metal in its structure. In general, Cbl has the most complex structure in comparison to other vitamins. Its structure is based on the corrin ring, which is a tetradentate heteromacrocycle that coordinates at the central cobalt ion through four nitrogen atoms. The α axial coordination position is occupied by the nitrogen atom from dimethylbenzamidazole. The sixth β coordination position at Co, trans to dimethylbenzoimidazole, is generally available only if the Co ion is in the 3+ oxidation state.[1,2] Cobalamin can exist in many forms, all resulting from changes in the oxidation state of the central ion. Cbl is a hexacoordinate complex with octahedral geometry for Co(III),[3] pyramidal pentacoordinate in the case of Co(II) and tetracoordinate with planar geometry for Co(I).[4,5] There are also some situations in which Cbl containing Co(II) is a hexacoordinate complex, but these are rare.[6,7]

* Corresponding author: radu.silaghi@ubbcluj.ro

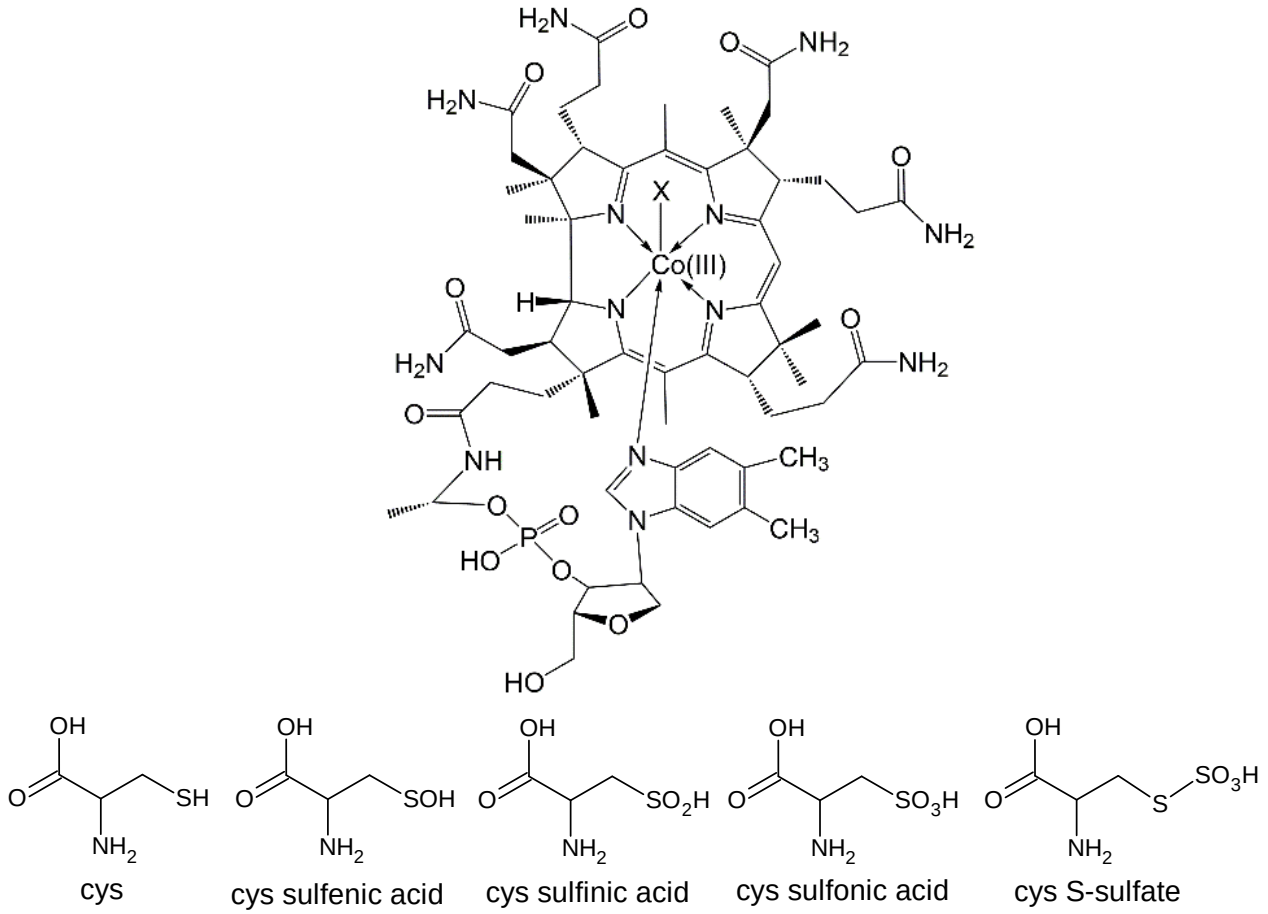

Fig. 1 – Top: structure of vitamin B_{12} (cobalamin). X is an exogenous ligand – which may be H_2O or HO^- (in aqua and hydroxo Cbl), alkyl (methyl or adenosyl, in physiological reaction intermediates of Cbl), cyanide (in cyanoCbl, the most common commercially-available form of Cbl), cysteine or its derivatives examined in the present study (as listed on the bottom row; fully neutral structures shown here – see Results for discussion of protonation states), or any number of small inorganic or organic ligands.

Cbl is the most widespread cobalt complex in vivo.[2] The biological functions of cobalamin are directly related to the oxidation state of the central ion.[8] There are two biologically active forms, methylcobalamin (MeCbl)[9] and adenosylcobalamin (AdoCbl).[10]

Cbl and its derivatives have attracted attention particularly because of the role in human physiology. The complexes formed by cobalamins are also of special interest to pharmacology as they proved to be useful in targeted drug delivery.[11] The MeCbl form is involved in the methyl transfer reaction with methyltransferase.[1213] The reactions catalyzed by Cbl revolve around the two types of reactions in which it can engage in. Vitamin B_{12}-catalyzed reactions are guided by two ways of Co-C bond cleaving. Heterolytic cleavage involves B_{12}-dependent methyl transferase, while homolytic cleavage involves B_{12}-dependent isomerases. The mechanism of methionine synthase is an example of a B_{12}-dependent enzyme that involves a heterolysis of the Co-C bond. This mechanism involves Co in the oxidation states +1 and +3;[14] Cbl (II) [15] can only occur accidentally, but there is an enzymatic mechanism that turns back the metal ion involved in the catalytic cycle to its initial oxidation state.[16] [17]

Cobalamin adducts are reported in the literature as species able to generate linkage isomers under biologically relevant conditions with ligands such as: NO, NO_2^-, O_2, H_2O_2 .[18] Among them, nitrosyl complexes are probably the most experimentally investigated due to their importance in the mediation of physiological effects that depend on nitric oxide. It is well known that cobalamins may act as scavengers of NO during septic shock when the amounts of released NO become harmful for the organism.[19,20]

In the reported literature, examples are available of cobalamin adducts in which a Co-S bound is formed with ligands such as HS^-, SO_3^{2-}, $S_2O_3^{2-}$, $HS_2O_3^-$, SCN^-.[21–25] Reactions with thiols like glutathione, homocysteine, L-cysteine and its derivatives give Cbl complexes in which the sulfur atom coordinates the Co^{3+} ion. If exposed to a strong acidic pH, these complexes hydrolyze back to

aquaCbl(III) and the corresponding thiol derivative. In contrast, the alkaline medium favors the reduction reaction to form Cbl(II). Monitoring of the formation of complexes between cobalamin and thiol derivatives is typically performed using UV-Vis spectroscopy. If compared to typical complexes which have ligands such as water, hydroxide or cyanide, major differences were identified which is why these spectra were named "atypical". In the typical UV-Vis spectra, the γ band, corresponding to the π-π * transitions from corrin is identified around 350 nm, while in the case of thiol complexes a bathochrome displacement and a decrease in intensity of this band are observed.[2,26,27]

Under biologically relevant conditions, cysteine can be oxidized at the sulfur by insertion of 1, 2 or 3 oxygen atoms – thus generating cysteine sulfenate, cysteine sulfenate and cysteic acid, respectively.[28–31] Cysteine sulfenate and sulfinate can still serve as ligands to biological metal centers – such as the Fe or the Co in nitrile hydratase, or the Co in cobalamin.[28–31]

Herein, we approach this subject with a different perspective by using new methods to reach to the core of the problem and we retrieved molecular models from three families of S-oxidized cysteine derivatives (cys-SO, cys-SO_2, cys-SO_3, alongside the more complex redox product, cys-S-SO_3). UV-vis measurements are complemented by DFT and TD-DFT calculations.

RESULTS AND DISCUSSIONS

The UV-vis spectra of the cysteine sulfinate and cysteine sulfenic acid adducts of Cbl were previously reported at pH 5.8 and 7.5–9.5, respectively.[28] Figure 2 shows spectra of Cbl mixed with cysteine sulfinate (cys-SO_2) and with its oxidized form cys-S-SO_3, confirming these previous results and offering a comparison with three reference ligands – sulfide, cysteine, and sulfite. These spectra confirm formation of complexes in all cases except cys-S-SO_3 and are essentially unaffected between pH 3 and 7 in line with previous observations;[28] at higher pH (10 or 12), where Cbl is present in a kinetically-inert Co(III)-hydroxo form, none of these ligands elicit changes in the spectrum of Cbl. Since cys-SO_2 and cys-S-SO_3 can in principle coordinate to the cobalt via sulfur or via oxygen, sulfite offers a reference consisting of a ligand capable of similar linkage isomerism. Sulfide (HS^-) offers a reference where coordination is guaranteed to occur via sulfur. Cysteine in principle could coordinate via any of its three functional groups (amino, carboxy, or thiolate), although extensive experimental evidence demonstrates that it only coordinates via the thiolate.[32] Not shown in Fig. 2 are reference spectra with acetate, diethylamine, and sulfate, which are identical with those of Cbl alone. Indeed, these latter three ligands are not reported in the literature to form a complex with Cbl.

Cysteine S-oxidized congeners offer the possibility of linkage isomerism when complexing Cbl – with the sulfur, the S-bound oxygen, the amino or the carboxy groups each capable in principle of coordination to cobalt. The fact that dimethylamine and acetate, but also especially cys-S-SO_3, do not elicit any change in the spectrum of Cbl may be taken as evidence against coordination of cys-SO_2 via the carboxy or the amino groups. The lack of coordination by cys-S-SO_3 is in line with the lack of coordination by sulfate: in both cases coordination via sulfur would be impossible sterically – and apparently coordination via a sulfur-bound oxygen atom is not thermodynamically feasible with these ligands. This latter observation also argues against the possibility of cys-SO_2 coordinating to Co via its sulfur-bound oxygen atom.

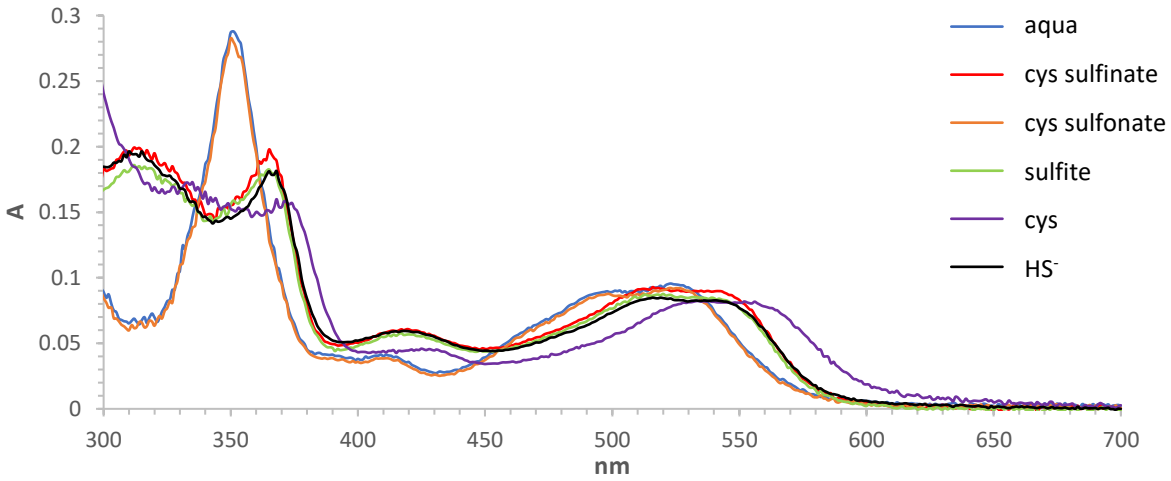

Fig. 2 – Comparison between UV-Vis spectra of Cbl adducts with cys derivatives and reference ligands.

Table 1 summarizes the experimental data on UV-vis spectra for various reference Cbl adducts vs. the cys-SO_2 adduct. Together with the data in Fig. 1 revealing a distinct similarity between the adducts of cys-SO_2 and HS^- and sulfite, but not with cysteine itself, this may be taken as evidence that cys-SO_2 coordinates to Cbl via its sulfur atom. Since no structural data is for now available to corroborate this conclusion, a computational study using density functional theory (DFT) was undertaken as detailed below.

Table 1

Experimental wavelengths and extinction coefficients ($M^{-1}\cdot cm^{-1}$) for the four main maxima in the UV-vis spectrum of Cbl variants examined in the present study and in the literature[33]

Adduct	Band I'	Band I	Band II	Band III	Band IV
Cbl-H_2O[33]	-	26500 (351 nm)	4200 (410 nm)	8800 (498 nm)	9500 (526 nm)
Cbl-OH[33]	-	21700 (358 nm)	4600 (419 nm)	9300 (514 nm)	10400 (535 nm)
Cbl-CN[33]	-	27500 (361 nm)	3500 (409 nm)	7600 (516nm)	8500 (550nm)
Cbl-cys	16015 (335 nm)	15167 (370 nm)	4185 (433 nm)	8093 (530 nm)	7398 (565 nm)
Cbl-βMT	16337 (335 nm)	14482 (370 nm)	4456 (433 nm)	8035 (530 nm)	7309 (565 nm)
Cbl-SH	21648 (311 nm)	20261 (367 nm)	6874 (420 nm)	10100 (516nm)	9820 (543 nm)
Cbl-cys-SO_2	18848 (330 nm)	21637 (353 nm)	3813 (426 nm)	8361 (510 nm)	7948 (543 nm)

Geometry optimization using DFT was first performed on cysteine S-oxidised derivatives (sulfenic, sulfinic, sulfonic and S-sulfate), exploring possible conformers with different protonation patterns that would mimic various pH values. The two possible tautomers for sulfenic and sulfinic acid were considered (-S(H)=O *vs*. -S-OH). In addition, complexes with a series of reference ligands were computed for reference: 2-mercaptoethanol (βMT), water, HO^-, acetate, cyanide, HS^-, CH_3S^-, NH_3. These complexes were generated using a truncated Cbl model that includes the corrin macrocycle with the central cobalt ion and imidazole in the axial position, α; for the sulfenic/sulfinic/sulfonic adducts, calculations on a full Cbl model (no truncation) were also performed. UV-vis spectra were computed using TD-DFT calculations.

Quantitative agreement between experiment and TD-DFT calculations is very rarely possible for metal complexes.[33,34] Qualitative or semi-quantitative agreement may be reached – but this requires a calibration of the method against standard known structures related to those for which new assignments are sought. Thus, in order to assign/ analyze the TD-DFT spectra of the Cbl complexes with cysteine and related derivatives, the UV-vis spectra were also simulated for three reference Cbl adducts: aqua, hydroxo and cyano. Several functionals were tested in order to generate a theoretical spectrum as close as possible to the experimental one for the three reference compounds. The TD-DFT data presented in this study are obtained using the B3PW91 functional, which provided the best agreement with the experimentally-observed trends when comparing aqua vs. hydroxo and *vs*. cyano Cbl, cf. Table 2.

The TD-DFT data in Table 2 reproduce the experimentally-observed trends in the ~510–530 nm plateaus of the aqua, hydroxo and cyano Cbl adducts: they are all grouped within ~20 nm of each other (500 – 521 nm), in the order of wavelengths aqua >> hydroxo > cyano. The adducts with ammonia or acetate, which are not observed experimentally but would mimic cysteine binding to cobalt via its amine or its carboxylate groups, are expectedly predicted to also show maxima within the same interval (516, 526 nm). Also, the mercaptoethanol isomers bound to Co via the oxygen atom do show maxima in the same region (523, 542 nm). However, all the thiolate complexes are predicted to have maxima at distinctly higher wavelengths – starting at 550 nm and going even higher for some protonation states. Similar trends are seen when examining the ~300 nm band – with similar bathochromic shifts of 10-20 nm in all thiolate complexes, in excellent agreement with experiment. Overall, these data confirm that cysteine binds to cobalamin via the (deprotonated) sulfur atom.

Table 3 shows TD-DFT data for the isomers of the cobalamin complex with cysteine sulfenate. Three protonation scenarios for the ligand are considered: 1 (neutral sulfenate group, neutral carboxyl, protonated -NH_3^+), 2 (same as 1, but now with the functional group coordinated to Co deprotonated), and 3 (neutral amine, deprotonated carboxylate and sulfenate).

Table 2

TD-DFT data for adducts of the truncated Cbl model with reference ligands. For βMT, two protonation states were considered: 1 (neutral ligand) and 2 (ligand deprotonated at the atom coordinated to the Co – either O or S). Experimental data (exp) derived from Table 1 is also shown (band I, and an average of the values for bands III and IV since the latter two are very close to each other in experiment while only a single band is predicted by TD-DFT in this region)

Adduct	Wavelength (nm)		Oscillator strength		Transition
	DFT	exp	DFT	exp	
Cbl-OH	521	524.5	0.2343	0.2433	HOMO-1 >LUMO+1
	358	358	0.4158	0.5359	HOMO-1 >LUMO+2
Cbl-H_2O	500	512	0.2515	0.2260	HOMO-1 >LUMO+1
	355	351	0.6356	0.6545	HOMO-1 >LUMO+5
Cbl-CN	520	533	0.2387	0.1988	HOMO-1 >LUMO+1
	359	361	0.6832	0.6792	HOMO-1 >LUMO+4
Cbl-NH_3	516	N.A.	0.2462	N.A.	HOMO-1 >LUMO+1
	359	N.A.	0.7389	N.A.	HOMO-1 >LUMO+4
Cbl-acetate	526	N.A.	0.2056	N.A.	HOMO-1 >LUMO+1
	360	N.A.	0.4429	N.A.	HOMO-1 >LUMO+4
Cbl-CH_3S	568	N.A.	0.1539	N.A.	HOMO-2 >LUMO+1
	376	N.A.	0.2869	N.A.	HOMO-4 >LUMO+1
Cbl-SH	553	529.5	0.1800	0.1913	HOMO-2 >LUMO+1 HOMO-1 >LUMO+1
	370	367	0.4746	0.3746	HOMO-2 >LUMO+3
Cbl-βMT-2-S	634	547.5	0.1059	0.1895	HOMO-2 >LUMO+3
	384	370	0.2684	0.3577	HOMO-4 >LUMO+3
Cbl-βMT-2-O	542	547.5	0.1716	0.1895	HOMO-4 >LUMO+1
	364	370	0.3418	0.3577	HOMO-4 >LUMO+3
Cbl-βMT-1-S	564	547.5	0.1560	0.1895	HOMO-2 >LUMO+1
	377	370	0.4268	0.3577	HOMO-2 >LUMO+3
Cbl-βMT-1-O	523	547.5	0.2033	0.1895	HOMO-2 >LUMO+1
	359	370	0.5515	0.3577	HOMO-2 >LUMO+3 HOMO-3 >LUMO+3

Table 3

TD-DFT maxima (with truncated Cbl models) and relative energies (d*E*, kcal/mol) for linkage isomers of Cbl complexed with cysteine sulfenate. Orbitals involved in these transitions are indicated (H = HOMO, L= LUMO). Relative energies are calculated within each protonation state for the three linkage isomers, taking as reference (0) the most stable isomer

Protonation model	Adduct	Wavelength (nm)	Oscillator strength	Transition	dE, truncated	dE, complete
1	Cbl-cys-S	525	0.1977	H-1 >L+1	0.6	8.5
		368	0.4461	H-1 >L+3		
	Cbl-cys-O	492	0.1958	H-2 >L+1	4.8	1.0
		351	0.5025	H-2 >L+3		
	Cbl-cys-COO	503	0.1869	H-1 >L+1	0.0	0.0
		357	0.4846	H-1 >L+4		
2	Cbl-cys-S	508	0.1777	H-2 >L+1	2.8	3.0
		355	0.2831	H-4 >L+2		
	Cbl-cys-O	504	0.1879	H-2 >L+1	0.0	0.0
		353	0.5899	H-2 >L+3		
	Cbl-cys-COO	531	0.1413	H-1 >L+1	3.7	10.9
		355	0.4502	H-2 >L+4		
3	Cbl-cys-S	508	0.1777	H-2 >L+1	7.9	14.7
		355	0.2831	H-4 >L+2		
	Cbl-cys-COO	503	0.1869	H-1 >L+1	10.1	-
		357	0.4846	H-1 >L+4		
	Cbl-cys-O	503	0.1970	H-5 >L+1	2.7	-
		351	0.3886	H-5 >L+3		
	Cbl-cys-NH_2	426	0.1200	H-4 >L+1	0.0	0.0
		361	0.3951	H-3 >L+3		

In the all-protonated scenario (1) of the Cbl-sulfenate adduct, the S- and carboxyl isomers are degenerate in energy within the truncated Cbl models, while in the full Cbl models the degeneracy is between the carboxyl and the S-bound oxygen. In the series (2) of models, where the cobalt-bound atom is now deprotonated (anionic), binding via the sulfenate oxygen is predicted to be favored energetically only slightly, by ~3 kcal/mol, compared to binding via the sulfur. In the all-deprotonated models (3), the amino group appears to be energetically favored. On the other hand, as shown above in Table 1, the experimentally-observed UV-vis spectra of the adducts of cysteine derivatives with cobalamin show similar but lower shifts vs. aqua Cbl, compared to those of the thiolate adducts. Since the TD-DFT-derived maxima of aquaCbl are at 351 and 512 nm, respectively, this comparison would rule out Cbl-sulfinate isomers bound via the sulfenate oxygen, for which Table 4 shows the ~350 nm band to remain essentially unmodified compared to the aqua adducts, in all three protonation states. Along the same lines, the amino isomer can be ruled out based on its predicted hypsochromic shift of the ~500-nm band. The wavelengths predicted for the carboxylate and the sulfur-bound isomers both fit with the experimental data. However, for the ~350-nm band the TD-DFT-predicted oscillator strengths of the carboxylate isomers are higher than those for the aqua complex, which is in disagreement with experiment and leaves only the sulfur-bound isomers to agree with experiment based on the TD-DFT data. This would imply an error of a few kcal/mol in the relative energies by DFT, which is not unprecedented.

In the case of cobalamin adducts models with the cysteine sulfinic derivative (Table 4), a difference correlated with the protonation model is observed. Truncated models from the first family of linkage isomers indicate the Cbl-S-cys isomer to be disfavored by 12.8 kcal/mol – with an even larger value in the complete model (20.9 kcal/mol). The SO- and COO-isomers are essentially energetically degenerate, at 0.1 kcal/mol within each other. On the other hand, the energy differences in the case of the complete model are higher: 14.2 kcal/mol. In this situation it is obvious that this energy difference is due to the intramolecular hydrogen bonds, because the binding of the oxygen attached to the sulfur implies the external exposure of the carboxyl favoring the hydrogen bonds with the cobalamin. In the second protonation mode, the truncated models favor the Cbl-S isomer by 4.0 kcal/mol compared to the Cbl-O isomer.

Table 4

TD-DFT maxima (from truncated Cbl models) and relative energies (d*E*, kcal/mol) for linkage isomers of Cbl complexed with cysteine sulfinate

Protonation model	Adduct	Wavelength (nm)	Oscillator strength	Transition	d*E*, truncated	d*E*, complete
1	Cbl-cys-S	526	0.2003	H-1 >L+1	12.8	20.9
		368	0.5744	H-2 >L+1		
	Cbl-cys-O	506	0.2288	H-1 >L+1	0.1	0.0
		356	0.5616	H-1 >L+4		
	Cbl-cys-COO	504	0.2322	H-1 >L+1	0.0	14.2
		355	0.5836	H-1 >L+4		
2	Cbl-cys-S	534	0.1722	H-1 >L+1	0.0	0.2
		368	0.2292	H-4 >L+1		
	Cbl-cys-O	504	0.1246	H-2 >L+1	4.0	0.0
		356	0.5102	H-1 >L+3		
	Cbl-cys-COO	515	0.2257	H-1 >L+1	5.4	7.8
		360	0.5344	H-1 >L+3		
3	Cbl-cys-S	536	0.1190	H-2 >L+1	1.3	19.3
		358	0.3742	H-6 >L+2		
	Cbl-cys-O	507	0.1977	H-3 >L+1	0.3	-
		348	0.3500	H-9 >L+2		
	Cbl-cys-COO	525	0.1535	H-2 >L+1	0.0	5.8
		362	0.1901	H-2 >L+4		
	Cbl-cys-NH_2	520	0.1700	H-2 >L+1	4.3	0.0
		373	0.2164	H-2 >L+2		
experimental		526.5	0.2014	-	-	-
		353	0.5344	-	-	-

For the full Cbl models, the oxygen-bound isomer is preferred by 0.2 kcal/mol. Such a small difference indicates the possibility of interconversion or coexistence of these two isomers under physiologically relevant conditions. Both models (truncated vs. full Cbl) indicate carboxylate coordination is thermodynamically disfavored, due to secondary interactions with nitrogen and oxygen atoms from the side chains of the corrin. Therefore, for the first protonation family, the highest stability of the Co-OS-cys isomer is predicted. In the second family of protonation, which is more relevant from the perspective of physiological conditions, the prevalence of the Co-S-cys isomer in real solutions may be concluded. Truncated models for the third protonation mode feature essentially identical energies for the SO-, COO- and S- linkage isomers (within ~1 kcal/mol from each other), followed closely by the amino isomer (~ 4.3 kcal mol).

In terms of the TD-DFT-derived UV-vis spectra, the S-bound isomer for scenario (2) (the experimentally-relevant variant, for the pH values where a cys-sulfinate-Cbl adduct was observed) is the only one reproducing the distinct bathochromic shift observed experimentally at ~500 nm as well as the hypochromism of the ~350 nm band. Since energetically this isomer is also favored, one can conclude a clear assignment of the experimental data: cysteine sulfinate binds to Co via the sulfur atom.

Sulfonic derivatives (Tables 5 and 6) are sterically unable to coordinate to Cbl via the sulfur atom of the SO_3 group.

Table 5

TD-DFT maxima (from truncated Cbl models) and relative energies (d*E*, kcal/mol) for linkage isomers of Cbl complexed with cysteine sulfonate

Protonation model	Adduct	Wavelength (nm)	Oscillator strength	Transition	d*E*, truncated	d*E*, complete
1	Cbl-cys-O	505	0.2355	L-1 >L+1	0.0	0.0
		354	0.6127	L-1 >L+4		
	Cbl-cys-COO	505	0.2355	L-1 >L+1	10.6	14.2
		354	0.6127	L-1 >L+4		
2	Cbl-cys-O	509	0.2255	L-1 >L+1	0.0	0.0
		356	0.5240	L-1 >L+4		
	Cbl-cys-COO	519	0.1934	L-1 >L+1	1.6	11.8
		361	0.4492	L-1 >L+4		
3	Cbl-cys-O	512	0.2003	L-2 >L+1	11.4	
		352	0.2530	L-2 >L+4		
	Cbl-cys-COO	527	0.1661	L-1 >L+1	0.0	0.0
		344	0.1942	L-2 >L+4		
	Cbl-cys-NH_2	546	0.1314	L-1 >L+1	1.7	11.1
		379	0.2343	L-1 >L+3		

Table 6

TD-DFT maxima (from truncated Cbl models) and relative energies (d*E*, kcal/mol) for linkage isomers of Cbl complexed with cysteine S-sulfate, cys-S-SO_3

Protonation model	Adduct	Wavelength (nm)	Oscillator strength	Transition	d*E*, truncated	d*E*, complete
1	Cbl-cys-S	528	0.1822	L-2 >L+1	10.6	12.4
		366	0.4374	L-1 >L+5		
	Cbl-cys-O	500	0.2304	L-1 >L+1	0.0	0.0
		356	0.4882	L-2 >L+4		
	Cbl-cys-COO	502	0.1889	L-1 >L+1	13.3	24
		357	0.5519	L-1 >L+5		
2	Cbl-cys-S	525	0.1810	L-1 >L+2	0.0	0.0
		363	0.3660	L-1 >L+5		
	Cbl-cys-O	507	0.2279	L-1 >L+1	3.4	0.3
		354	0.5505	L-8 >L+1		
	Cbl-cys-COO	509	0.2261	L-1 >L+2	1.8	2.0
		356	0.5690	L-1 >L+5		
3	Cbl-cys-S	532	0.1871	L-1 >L+1	7.4	20.4
		367	0.3121	L-1 >L+5		
	Cbl-cys-O	507	0.1787	L-3 >L+2	21.8	-
		354	0.4370	L-3 >L+4		
	Cbl-cys-COO	529	0.1259	L-1 >L+1	0.0	-
		355	0.2050	L-1 >L+3		
	Cbl-cys-NH_2	525	0.1812	L-1 >L+1	0.2	0.0
		361	0.1527	L-8 >L+1		

For cys-SO_3, in the first protonation mode, the most stable isomer is predicted to be the Cbl-O-cys in both models of cobalamin, by more than 10 kcal/mol. The trend is maintained, though with lower energy differences, in the second family of protonated models. For cys-S-SO_3 (cysteine S-sulfate), truncated models for the first protonation family favor the Cbl-O-S adduct, followed by the adduct formed through the S atom of the disulfide bridge at 10.6 kcal/mol. In the first family of isomers, the Cbl-O-cys isomer is energetically favored, the two remaining isomers are energetically far apart. From the structural point of view, the Cbl-S isomer is sterically disadvantaged due to the voluminous groups attached to the sulfur atom in the bridge. This trend is sustained by the complete models for the first protonation family, by increasing the energetic difference between the Cbl-COO/O isomers. In the case of the second protonation model, the S-isomer is energetically favored for both the truncated and complete models of Cbl, though the SO- isomer is also very close in energy (0.3 kcal/mol). Completely deprotonated models indicate the possibility of coexistence of Cbl-COO / NH_2 isomers with an energy difference of 0.2 kcal / mol. Overall, these data suggest that if coordination is to occur with cys-SO_3 or cys-S-SO_3, it would be via the carboxyl or amino groups. These data are, however, computed for isolated molecules, not accounting for the 55 M concentration of water molecules in buffer solutions; since we know experimentally that such functional groups are unable to coordinate to Cbl under normal aqueous conditions, one may conclude that there is a reasonable agreement with experiment.

EXPERIMENTAL

Aqua cobalamin hydrochloride (HOCbl ≥ 98 %) and the ligands cysteine, Na_2SO_3, Na_2SO_4, β-mercaptoethanol (β-MT), diethylamine, ammonia, sodium sulfide and sodium acetate were purchased from Sigma Aldrich. 50 mM solutions of mono-, di- and trisodic phosphate in bidistilled water were prepared, titrated to the desired pH value (3, 5, 7, 10 and 12 respectively) and used as buffers.

Calculations were carried out with DFT[35] and TD-DFT methods using the TPSS[36] density functional and the Gaussian 9 software package.[37] Two molecular models (complete and truncated) for cobalamin were generated. In the truncated model, the lateral substituents on the corrin as well as the methyl groups on the benzimidazole replaced by hydrogen atoms. Gas-phase geometries and frequency analyses of ligands were computed with the aid of the B3LYP[38] functional with the def2-SV(P) double-zeta basis set. TD-DFT derived[39] UV-Vis spectra were computed in the C-PCM solvent continuum adapted for aqueous environment.[40] For the latter property, the B3PW91[38,41] functional was employed. From the TD-DFT outputs, reported here are the most intense transition in the visible region (equivalent to Bands III and IV in Table 1) and the most intense band in the 300-400 nm region. The wavelengths and oscillator strengths for these two maxima are reported in Tables 2-6 after scaling, since as discussed before[33] the agreement with experiment is only semi-quantitative and would be difficult to follow without scaling. Thus, for oscillator strengths (*f*) the scaling formula was $f_{reported} = = f_{TDDFT} \cdot 1.9677$. For the wavelengths, the formulae were $\lambda_{Band\ I,\ reported} = 42.10 + \lambda_{Band\ I,\ TDDFT}$ and $\lambda_{Band\ III+IV,\ reported} = 42.10 + \lambda_{Band\ I,\ TDDFT} + (\lambda_{Band\ III+IV,\ TDDFT} - \lambda_{Band\ I,\ TDDFT})^{1.0370}$. The numerical coefficients in these scaling equations were derived from least-squares fitting procedures against experimental data for aqua, hydroxo, cyano and sulfido Cbl shown in Table 1. Interconversion between oscillator strength f and molar absorptivity ε was performed using the formula $\varepsilon = 40490 \cdot f$, which assumes a value of 0.4 eV (as typical in GaussView) for the half-width of the Gaussian band at $\varepsilon = \varepsilon_{max}/e$.[37]

UV-vis spectra were recorded on a Cary 50 UV-vis spectrophotometer (Varian, Inc., Foster City, CA, USA) and were monitored for up to 65 minutes after mixing Cbl with its potential ligands to verify the stability of the final products. Unless otherwise specified, the aquaCbl was at a concentration of 0.017 mM, with the ligand at an excess of × 100.

CONCLUSIONS

UV-Vis spectroscopy corroborated by DFT calculations was employed to confirm the formation of new adducts of Co(III) cobalamin with cysteine and cysteine sulfinic acid. Linkage isomerism is suggested to be possible in several cases based on relative energy differences of less than 5 kcal/mol as computed from DFT calculations – with coordination thus possible by other atoms than the sulfur. However, the fact that the experimental data only shows S- coordination suggests that the competition from water molecules/ligands is too strong and the Co-oxygen/nitrogen bonds in the respective linkage isomers are too kinetically labile to be observed experimentally in aqueous environments. Experimental examination in non-coordinating solvents is in this case expected to reveal coordination of cysteine and of its congeners via oxygen and/or nitrogen ligands as well.

Acknowledgements. Funding from Funding from the Romanian Ministry of Education and Research (project PN-III-P4-ID-PCCF-2016-0142) is gratefully acknowledged. Prof. S. V. Makarov (Ivanovo State University of Chemistry and Technology) is thanked for helpful discussions.

REFERENCES

1. F. Zelder, K. Zhou and M. Sonnay, *Dalt. Trans.* **2013**, *42*, 854–862. https://doi.org/10.1039/C2DT32005C.

2. I. A. Dereven'kov, D. S. Salnikov, R. Silaghi-Dumitrescu, S. V. Makarov and O. I. Koiffman, *Coord. Chem. Rev.* **2016**, *309*, 68–83. https://doi.org/10.1016/j.ccr.2015.11.001.
3. B. Kräutler, *Chem. – A Eur. J.*, **2015**, *21*, 11280–11287. https://doi.org/10.1002/chem.201502072.
4. M. Giorgetti, I. Ascone, M. Berrettoni, P. Conti, S. Zamponi and R. Marassi, *JBIC J. Biol. Inorg. Chem.*, **2000**, *5*, 156–166. https://doi.org/10.1007/s007750050360.
5. B. Kräutler, *Biochem. Soc. Trans.* **2005**, *33*, 806–810. https:// doi.org/10.1042/BST0330806.
6. D. S. Salnikov, R. Silaghi-Dumitrescu, S. V. Makarov, R. van Eldik and G. R. Boss, *Dalt. Trans.*, **2011**, *40*, 9831–9834.
7. I. A. Dereven'kov, P. A. Ivlev, C. Bischin, D. S. Salnikov, R. Silaghi-Dumitrescu, S. V. Makarov and O. I. Koifman, *J. Biol. Inorg. Chem.*, **2017**. https://doi.org/10.1007/s00775-017-1474-z.
8. C. Gherasim, M. Lofgren and R. Banerjee, *J. Biol. Chem.*, **2013**, *288*, 13186–13193. https://doi.org/10.1074/jbc.R113.458810.
9. H. Fang, J. Kang and D. Zhang, *Microb. Cell Fact.*, **2017**, *16*, 15. https://doi.org/10.1186/s12934-017-0631-y.
10. J. Marie Sych, C. Lacroix and M. J. A. Stevens, "Vitamin B12 – Physiology, Production and Application", in "Industrial Biotechnology of Vitamins, Biopigments, and Antioxidants", Wiley-VCH Verlag GmbH & Co. KGaA: Weinheim, Germany, 2016, p. 129–159. https://doi.org/ 10.1002/ 9783527681754.ch6.
11. D. Rutkowska-Zbik, M. Jaworska and M. Witko, *Struct. Chem.*, **2004**, *15*, 431–435. https://doi.org/10.1023/ B:STUC.0000037900.67595.9f.
12. R. G. Matthews, M. Koutmos and S. Datta, *Curr. Opin. Struct. Biol.*, **2008**, *18*, 658–666. https://doi.org/10.1016/ j.sbi.2008.11.005.
13. R. G. Matthews, "2 Cobalamin- and Corrinoid-Dependent Enzymes", in "Metal-Carbon Bonds in Enzymes and Cofactors", DE GRUYTER, 2015; p 53–114. https://doi.org/10.1515/ 9783110436587-006.
14. M. Giedyk, K. Goliszewska and D. Gryko, *Chem. Soc. Rev.*, **2015**, *44*, 3391–3404. https://doi.org/10.1039/C5CS00165J.
15. S.-L. Chen, M. R. A. Blomberg and P. E. M. Siegbahn, *J. Phys. Chem., B* **2011**, *115*, 4066–4077. https:// doi.org/10.1021/jp105729e.
16. Y. Hisaeda, T. Nishioka, Y. Inoue, K. Asada and T. Hayashi, *Coord. Chem. Rev.*, **2000**, *198*, 21–37. https://doi.org/10.1016/S0010-8545(99)00222-2.
17. R. Silaghi-Dumitrescu, *An Introduction to Bioinorganic Chemistry*, Presa Universitara Clujeana, Cluj-Napoca, 2015.
18. M. Surducan, S. V. Makarov and R. Silaghi-Dumitrescu, *Polyhedron*, **2014**, *78*, 72–84. https://doi.org/10.1016/ j.poly.2014.03.009.
19. M. Brouwer, W. Chamulitrat, G. Ferruzzi and D. Sauls, J. Weinberg, *Blood*, **1996**, *88* (5), 1857–1864. https://doi.org/10.1182/ blood.V88.5.1857.bloodjournal8851857.
20. H. Kruszyna, J. S. Magyar, L. G. Rochelle, M. A. Russell, R. P. Smith and D. E. Wilcox, *J. Pharmacol. Exp. Ther.*, **1998**, *285*, 665–671.
21. K. Tahara, A. Matsuzaki, T. Masuko, J. Kikuchi and Y. Hisaeda, *Dalt. Trans.*, **2013**, *42*, 6410. https://doi.org/ 10.1039/ c3dt00042g.
22. D. S. Salnikov, P. N. Kucherenko, I. A. Dereven'kov, S. V. Makarov and R. van Eldik, *Eur. J. Inorg. Chem.*, **2014**, *2014* (5), 852–862. https:// doi.org/10.1002/ejic.201301340.
23. I. A. Dereven'kov, D. S. Salnikov, S. V. Makarov, G. R. Boss and O. I. Koifman, *Dalt. Trans.*, **2013**, *42*, 15307. https://doi.org/10.1039/c3dt51714d.
24. Y. Fujita, Y. Fujino, M. Onodera, S. Kikuchi, T. Kikkawa, Y. Inoue, H. Niitsu, K. Takahashi and S. Endo, *J. Anal. Toxicol.*, **2011**, *35*, 119–123. https://doi.org/10.1093/anatox/35.2.119.
25. I. A. Dereven'Kov, D. S. Salnikov, S. V. Makarov, M. Surducan, R. Silaghi-Dumitrescu and G. R. R. Boss, *J. Inorg. Biochem.*, **2013**, *125*, 32–39. https:// doi.org/10.1016/j.jinorgbio.2013.04.011.
26. F. Nome and J. H. Fendler, *J. Chem. Soc. Dalt. Trans.*, **1976**, *13*, 1212. https:// doi.org/10.1039/dt9760001212.
27. A. S. Eisenberg, I. V. Likhtina, V. S. Znamenskiy and R. L. Birke, *J. Phys. Chem.*, **2012**, *116*, 6851–6869. https://doi.org/10.1021/jp301294x.
28. I. A. Dereven'kov, L. V. Tsaba, E. A. Pokrovskaya and S. V. Makarov, *J. Coord. Chem.*, **2018**, *71*, 3194–3206. https:// doi.org/10.1080/00958972.2018.1515927.
29. A. Claiborne, J. I. Yeh, T. C. Mallett, J. Luba, E. J. Crane 3rd, V. Charrier, D. Parsonage, E. J. Crane 3rd, V. Charrier and D. Parsonage, *Biochemistry*, **1999**, *38*, 15407–15416.
30. A. Claiborne, T. C. Mallett, J. I. Yeh, J. Luba and D. Parsonage, *Adv. Protein. Chem.*, **2001**, *58*, 215–276.
31. R. Silaghi-Dumitrescu, *Rev. Chim.*, **2005**, *56*, 359–362.
32. R. K. Suto, N. E. Brasch, O. P. Anderson and R. G. Finke, *Inorg. Chem.*, **2001**, *40*, 2686–2692. https://doi.org/10.1021/ic001365n.
33. M. Lehene, D. Plesa, S. Ionescu-Zinca, S. D. Iancu, N. Leopold, S. V. Makarov, A. M. V. Brânzanic and R. Silaghi-Dumitrescu, *Inorg. Chem.*, **2021**, *60*, 12681–12684. https://doi.org/10.1021/acs.inorgchem.1c01483.
34. A. A. A. Attia, D. Cioloboc, A. Lupan, and R. Silaghi-Dumitrescu, *J. Inorg. Biochem.*, **2016**, *165*, 49–53. https:// doi.org/10.1016/j.jinorgbio.2016.09.017.
35. D. R. Salahub, A. de la Lande, A. Goursot, R. Zhang and Y. Zhang, "Recent Progress in Density Functional Methodology for Biomolecular Modeling", in "Structure iand Bonding", 2013, Vol. 150, p. 1–64. https://doi.org/ 10.1007/978-3-642-32750-6_1.
36. M. Bühl and H. Kabrede, *J. Chem. Theory Comput.*, **2006**, *2*, 1282–1290. https://doi.org/ 10.1021/ct6001187.
37. M. J. Frisch, G. W. Trucks, H. B. Schlegel, G. E. Scuseria, M. A. Robb, J. R. Cheeseman, G. Scalmani, V. Barone, B. Mennucci, G. A. Petersson, "Gaussian 09", Revision A. 02, Gaussian, Inc., Wallingford, CT, 2009, 2015.
38. A. D. Becke, *J. Chem. Phys.*, **1993**, *98*, 5648–5652. https://doi.org/10.1063/1.464913.
39. C. Lee, W. Yang and R. G. Parr, *Phys. Rev., B* **1988**, *37*, 785–789. https://doi.org/10.1103/PhysRevB.37.785.
40. A. Schäfer, H. Horn and R. Ahlrichs, *J. Chem. Phys.*, **1992**, *97*, 2571–2577. https://doi.org/ 10.1063/1.463096.
41. J. P. Perdew and Y. Wang, *Phys. Rev., B* **1992**, *46*, 12947–12954.